ELSEVIER

Physica D 84 (1995) 1–11

PHYSICA D

Turing structures. Progress toward a room temperature, closed system

Irving R. Epstein, István Lengyel

Department of Chemistry and Center for Complex Systems, Brandeis University, Waltham, MA 02254-9110, USA

Abstract

There are many parallels between the study of temporal oscillation in homogeneous chemical systems and of Turing patterns in reaction–diffusion systems. We discuss recent progress toward constructing a system that displays Turing structures under conditions suitable for a lecture demonstration. Such a system would play a role similar to that of the Belousov–Zhabotinsky oscillating reaction. We examine the prototype chlorite–iodide–malonic acid and related reactions, mathematical models, methods for designing new reactions that exhibit Turing structures and an approach to generating Turing structures in a closed system.

1. Introduction

The phenomenon of Turing structure formation, the spontaneous emergence in a reaction–diffusion system of a stable, stationary, spatially inhomogeneous, symmetry-breaking state from an initially homogeneous stationary state, has received considerable attention since the first experimental demonstration in 1990 [1] of Turing structures in a simple chemical reaction. Unlike oscillating chemical reactions, however, where the availability of several easily prepared lecture demonstrations [2] made the phenomenon accessible to essentially any interested chemist, few scientists have actually seen a "live" Turing pattern. The unstirred flow reactors utilized by a handful of research groups [1,3,4] to study Turing patterns are difficult to build and maintain and do not lend themselves to lecture demonstrations. The ultrahigh vacuum technology required for experiments on catalysis of carbon monoxide oxidation by single crystals of platinum, the other experimental system where Turing structures have been observed [5], is extremely costly and unwieldy.

We summarize here recent developments in our laboratory aimed at characterizing and understanding the Turing phenomenon in prototype systems and, ultimately, at developing systems that can be used for Turing experiments without need of special apparatus. We look first at the prototype chlorite–iodide–malonic acid (CIMA) reaction, the empirical rate law that describes its kinetics, a simple two-variable model derived from that rate law, and a chemical variant of the CIMA reaction that facilitates comparison between experimental and model Turing patterns. With insights gained from our mechanistic analysis, we examine the question of whether it should be possible to design new systems that exhibit Turing structures.

We next consider an important geometric

0167-2789/95/$09.50
SSDI 0167-2789(95)00003-8

aspect of the experiments to date, that Turing patterns have been studied as essentially two-dimensional patterns in a three-dimensional medium. What determines the location of the pseudo-two-dimensional structure within the medium? More importantly, what conditions are required for the structures to appear in two rather than in three dimensions? The answers to these questions suggest an approach by which transient Turing structures can be obtained in a closed system, bringing us closer to our goal of a convenient configuration for demonstrating the Turing phenomenon. We conclude by suggesting directions in which we think this field is likely to evolve.

2. The CIMA system

The chemical reaction in which experimental evidence of Turing structures was first found is the chlorite–iodide–malonic acid reaction, one of the few chemical oscillators that exhibits sustained temporal oscillation in a closed (batch) system [6]. While the chemistry of the core chlorite–iodide subsystem had been thoroughly studied [7–10], the mechanism of the full reaction including malonic acid (MA) was not illuminated until shortly after the discovery of Turing structures in the system. Both Epstein and Orbán [11] and Rábai and Beck [12] had pointed to chlorine dioxide, ClO_2, as a species that, while not included in the original chlorite–iodide mechanisms [10], merited further consideration in the chlorite–iodide and related systems. Our analysis of the CIMA reaction revealed [13] that chlorine dioxide and molecular iodine (I_2) were key species in both the temporal oscillation and the Turing behavior. We proposed an empirical rate law model consisting of three overall processes:

$$\mathrm{MA} + \mathrm{I_2} \rightarrow \mathrm{IMA} + \mathrm{I^-} + \mathrm{H^+}\,, \quad r_1 = \frac{k_{1a}[\mathrm{MA}][\mathrm{I_2}]}{k_{1b} + [\mathrm{I_2}]}\,,$$

$$\mathrm{ClO_2} + \mathrm{I^-} \rightarrow \mathrm{ClO_2^-} + \tfrac{1}{2}\mathrm{I_2}\,, \quad r_2 = k_2[\mathrm{ClO_2}][\mathrm{I^-}]\,,$$

$$\mathrm{ClO_2^-} + 4\mathrm{I^-} + 4\mathrm{H^+} \rightarrow 2\mathrm{I_2} + \mathrm{Cl^-} + 2\mathrm{H_2O}\,,$$

$$r_3 = k_{3a}[\mathrm{ClO_2}][\mathrm{I^-}][\mathrm{H^+}] + \frac{k_{3b}[\mathrm{ClO_2}][\mathrm{I_2}][\mathrm{I^-}]}{u + [\mathrm{I^-}]^2}\,. \tag{1}$$

The values of the parameters are [13]: $k_{1a} = 7.5 \times 10^{-3}\ \mathrm{M^{-1}\,s^{-1}}$ and $k_{1b} = 5 \times 10^{-5}$ M at pH = 2, $k_2 = 6 \times 10^{3}\ \mathrm{M^{-1}\,s^{-1}}$, $k_{3a} = 460\ \mathrm{M^{-2}\,s^{-1}}$, $k_{3b} = 2.65 \times 10^{-3}\ \mathrm{s^{-1}}$ and $u = 10^{-14}\ \mathrm{M^2}$ at 25°C and the activation parameters are $E_{1a} = 81.5$, $E_2 = 62.0$, $E_{3a} = 51.4$ and $E_{3b} = 110.0\ \mathrm{kJ\,mol^{-1}}$ [14].

Such empirical rate law models succeed only when the intermediates of the component overall processes do not interact with one another to any significant degree. If cross-reactions between intermediates are present, then a full elementary step mechanism is required. The comparison of simulated and experimental oscillatory behavior shown in Fig. 1 suggests that in this case the empirical rate law approach works quite well.

Our numerical studies show that when Eqs. (1) are integrated to give oscillatory behavior, the concentrations of chlorine dioxide, iodine and malonic acid change relatively little during each oscillatory cycle, while those of chlorite and iodide undergo large amplitude variations. These simulations with the full model suggest that it might be possible to describe the reaction with a simpler model in which only $[\mathrm{ClO_2^-}]$ and $[\mathrm{I^-}]$ are taken as variables and the concentrations of ClO_2, I_2 and MA are fixed. Experimental support for this approach is provided by experiments in which these latter three species are used as the starting materials in a batch reaction. We observe oscillations with the same waveform and frequency as in the CIMA system, but without any induction period.

The reduced model consists of the following "reactions", where X represents iodide and Y is chlorite ion:

$$\rightarrow \mathrm{X}\,, \quad r_1 = k_1'\,, \quad k_1' = k_{1a}[\mathrm{MA}]_0\,,$$

$$\mathrm{X} \rightarrow \mathrm{Y}\,, \quad r_2 = k_2'[\mathrm{X}]\,, \quad k_2' = k_2[\mathrm{ClO_2}]_0\,,$$

$$4\mathrm{X} + \mathrm{Y} \rightarrow \mathrm{P}\,, \quad r_3 = k_3'\frac{[\mathrm{X}][\mathrm{Y}]}{u + [\mathrm{X}]^2}\,, \quad k_3' = k_{3b}[\mathrm{I_2}]_0\,. \tag{2}$$

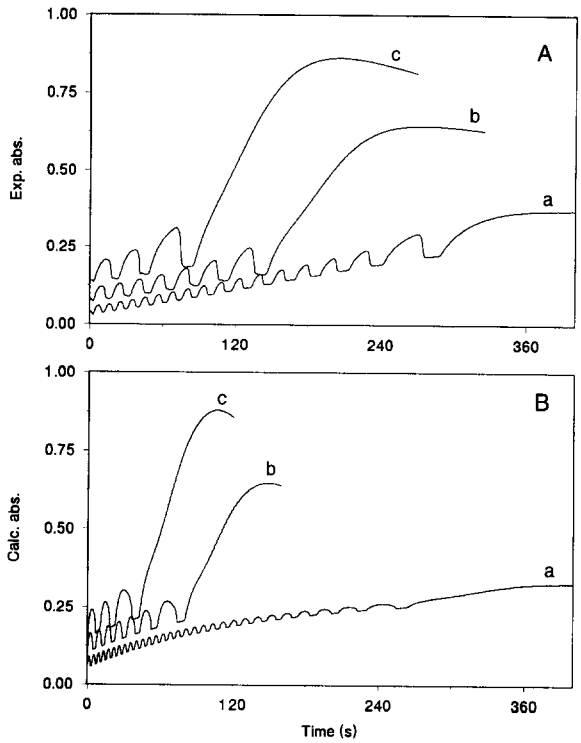

Fig. 1. Experimental (A) and calculated (B) oscillations in absorbance (280 nm) in the ClO_2–I_2–MA reaction. $[ClO_2]_0 = 1.7 \times 10^{-4}$ (a), 1.0×10^{-4} (b), 7.1×10^{-5} (c), $[I_2]_0 = 5.0 \times 10^{-4}$, $[MA]_0 = 1.0 \times 10^{-3}$, $[H_2SO_4] = 5.0 \times 10^{-3}$ M. For clarity, curves b and c have been shifted upward by 0.05 and 0.10 absorbance units, respectively, since in the absence of a shift the curves overlap significantly.

The differential equation system becomes

$$\frac{d[X]}{dt} = k_1' - k_2'[X] - 4k_3' \frac{[X][Y]}{u + [X]^2},$$

$$\frac{d[Y]}{dt} = k_2'[X] - k_3' \frac{[X][Y]}{u + [X]^2}. \tag{3}$$

On introducing scaled variables and constants we can put the resulting system of differential equations into dimensionless form:

$$\frac{dx}{d\tau} = a - x - 4\frac{xy}{1 + x^2},$$

$$\frac{dy}{d\tau} = b\left(x - \frac{xy}{1 + x^2}\right), \tag{4}$$

where

$$x = \frac{[X]}{\sqrt{u}}, \quad y = [Y]\frac{k_3'}{k_2' u}, \quad \tau = k_2' t,$$

$$a = \frac{k_1'}{k_3'\sqrt{u}}, \quad b = \frac{k_2'}{k_3'\sqrt{u}}. \tag{5}$$

The steady state solution of this system is $u_{SS} = a/5$, $v_{SS} = 1 + a^2/25$. The stable steady state loses its stability through a Hopf bifurcation if

$$b < \frac{3a}{5} - \frac{25}{a}. \tag{6}$$

The Poincaré–Bendixson theorem [15] guarantees that under these conditions the system will have a periodic limit cycle solution. The experimental range of oscillation is well described by this equation, except when the initial concentration of ClO_2 is so low that it is nearly consumed in one oscillatory period, violating the assumption that $[ClO_2]$ is a constant.

In order to understand Turing structure formation in the CIMA system, one other factor must be taken into account. If one simply adds diffusion terms to the rate equations (4) and makes the reasonable assumption that the diffusion constants of chlorite and iodide are roughly equal, no Turing structures result. An important outcome of Turing's analysis [16,17] is that the ratio of the diffusion constants of the activator (in this case iodide) and the inhibitor (here chlorite) must exceed a value determined by the kinetic parameters of the system. In the CIMA reaction, and in most chemical reactions, this value is significantly greater than unity, generally in the range 5–20. In aqueous solution, nearly all monomeric species have diffusion constants within about a factor of two of 2×10^{-5} $cm^2 s^{-1}$. This fact accounts for the lengthy gap in time between Turing's 1952 description of these patterns and their first experimental discovery in 1990.

The Turing structures in the CIMA system result from a fortunate coincidence. In order to enhance the contrast between the reduced and oxidized regions of the system, Castets et al. [1] used starch as an indicator. In the presence of the relatively high concentrations of I_2 present in

the CIMA system, the starch, S, forms a quite stable complex with iodine and the activator iodide species:

$$S + I^- + I_2 \rightleftharpoons SI_3^-, \quad K = \frac{[SI_3]}{[S][I_2][I^-]}. \tag{7}$$

The starch-triiodide complex, SI_3^-, is essentially immobile. Thus, the diffusion of the iodide is effectively slowed by its capture in the SI_3^- complex as it moves through the gel medium of the unstirred flow reactor (CFUR) in which the experiments are conducted. If we define $K' = K[S][I_2]$, then Eqs. (4) become

$$\frac{dx}{d\tau'} = a - x - 4\frac{xy}{1+x^2} + \frac{\partial^2 y}{\partial z^2},$$

$$\frac{dy}{d\tau'} = (1+K')\left[b\left(x - \frac{xy}{1+x^2}\right) + c\frac{\partial^2 y}{\partial z^2}\right], \tag{8}$$

where $\tau' = (1+K')\tau$, $K' = K[S]_0[I_2]_0$, c is the ratio of diffusion coefficients of chlorite and iodide ions and z is the spatial coordinate. The relevant ratio of diffusion constants thus becomes $(1+K')c$ rather than c. Since K' can be increased by varying the starch concentration, it is possible to achieve ratios considerably higher than unity.

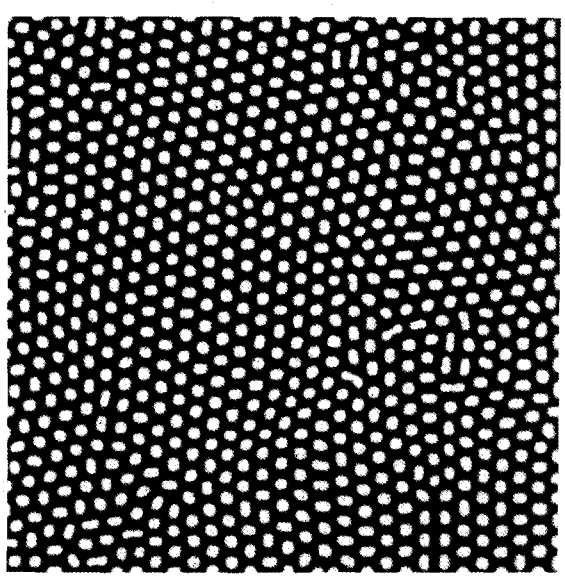

Fig. 2. Calculated Turing pattern from Eq. (8). $a = 36.0$, $b = 2.8$, $c = 1.2$, $K' = 8.0$. Number of gridpoints 320×320 in a total length of 160 dimensionless units. Periodic boundary conditions were applied to decrease the effect of the boundary on the patterns.

Integration of the "Brandeisator" (8) with realistic values of the parameters yields Turing patterns very similar to those observed in the CIMA system. One such pattern is shown in Fig. 2. To test these predictions experimentally, we carried out experiments, not with the CIMA reaction used in earlier studies, but with the chlorine dioxide–iodine–malonic acid (CDIMA) reaction that is actually described by the model equations. The results of two experiments are shown in Fig. 3.

3. Designing new Turing systems

One of the most significant developments in nonlinear chemical dynamics during the 1980s was the discovery of literally dozens of new oscillating reactions through the use of a systematic search procedure or design algorithm. At present, only the CIMA and CDIMA systems have been shown to exhibit Turing patterns, but our analysis of the role of starch in these systems suggests a route toward designing further such systems.

We focus on the role of the starch in solving the problem of making the activator diffuse much more slowly than the inhibitor, and we attempt to generalize that role. Our proposed design algorithm is as follows [18].

We first select a chemical oscillator that oscillates either in batch or at a relatively low flow rate in a stirred tank reactor (CSTR). All known experimental and model systems that exhibit Turing structures also show temporal oscillations for other sets of parameters. The low flow rate is necessary because it is impossible to achieve as high a flow rate through a gel reactor as through a CSTR. We must then identify the activator and inhibitor species in the system and find a complexing agent that reversibly forms a relatively

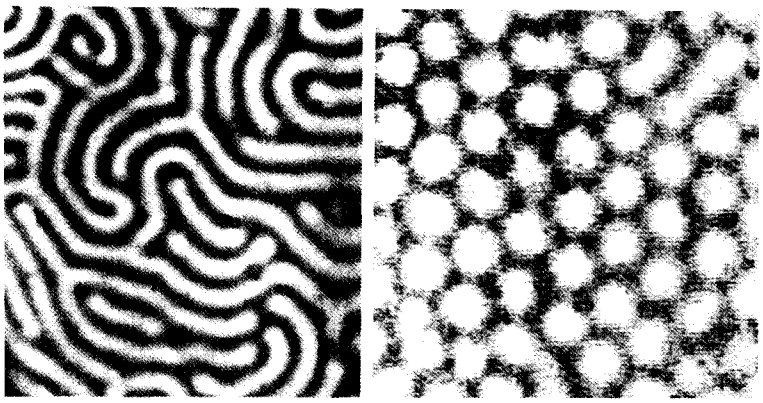

Fig. 3. Quasi-two-dimensional Turing patterns in the CDIMA reaction. Feed concentrations: stripes, $[MA]_0 = 1.0 \times 10^{-2}$ M, $[ClO_2]_0 = 1.5 \times 10^{-3}$ M at one end, $[I_2]_0 = 8.0 \times 10^{-4}$ M at other end; dots, $[MA]_0 = 2.0 \times 10^{-2}$ M, $[ClO_2]_0 = 1.0 \times 10^{-3}$ M at one end, $[I_2]_0 = 8.0 \times 10^{-4}$ M at other end. The wavelength of the structures is approximately 0.2 mm in both pictures.

stable, unreactive and immobile complex with the activator. This complex plays the role of the starch–triiodide complex in the CIMA reaction, slowing the diffusion of the activator. Experiments are carried out on the stirred system, adding increasing amounts of the complexing agent to establish how much is necessary to suppress oscillations and stabilize the homogeneous steady state to homogeneous perturbations. The next step requires running the reaction in an open CFUR, in which the gel has been made up to incorporate the complexing agent. The reagents are fed in from opposite ends of the reactor in such a way that no reaction occurs until the reagents diffuse together in the interior of the gel. The final step requires adjusting the concentrations of the complexing agent and/or of the input reagents to obtain Turing patterns.

Other than in the CDIMA system, which is only a minor variant of the CIMA reaction, this procedure has not yet been implemented experimentally. Promising systems include the mixed Landolt or EOE reaction [19] of iodate, sulfite and ferrocyanide, which has recently been used to generate a variety of spatiotemporal patterns in a CFUR [20], and the family of pH-regulated oscillators [21], where it should be possible to complex the activator hydrogen ion with a macromolecular base that can also serve as a color indicator.

4. Two- and three-dimensional structures

The Turing structures observed experimentally to date all occur in a single two-dimensional layer. This fact is both fortunate, since it facilitates optical measurements, and surprising, since typically the wavelength of the structures is about 0.2 mm and the gel layer in which they form is more than 1 mm thick. Intuitively, one might argue that the Turing structures arise only in a thin layer because of the geometry of the experiment. In a CFUR, as shown schematically in Fig. 4, reagents are fed in from opposite sides of the gel rather than being uniformly dispersed throughout the medium as envisioned by Turing. There is thus a significant gradient across the medium in each of the feed reactant concentrations. It is plausible that the set of concentrations that allows for Turing pattern formation occurs only within a relatively thin layer perpendicular to the direction of flow. Can this notion be made more precise?

Given a model for the chemistry of a system, linear stability analysis yields two conditions for

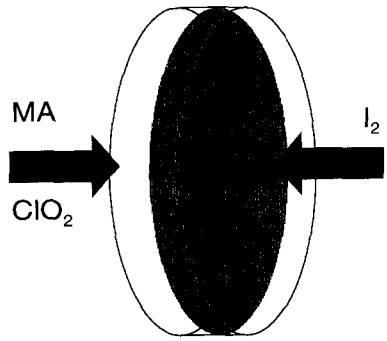

Fig. 4. Schematic diagram of reactant feeds into the gel in an experiment to study Turing patterns in the CDIMA reaction.

Turing pattern formation. These conditions can be expressed as inequalities involving the rate and diffusion constants, the concentrations of constant species and the steady state concentrations of the variable species. One condition specifies that the homogeneous steady state be stable to homogeneous perturbations; the other requires that this state be unstable to at least one inhomogeneous perturbation.

We have derived these expressions [22] for the dimensioned form of model of Eqs. (8). The pair of inequalities obtained may be written as

$$K' > H_1 > H_2 , \tag{9}$$

where $H_1 = -a_{11}/a_{22} - 1$, $H_2 = -a_{11}/(2(c(a_{11}a_{22} - a_{12}a_{21}))^{1/2}) - 1$, a_{ij} are the elements of the Jacobian matrix of the complex-free system and c is the ratio of the diffusion coefficient of the inhibitor to that of the activator. Because the a_{ij} are concentration dependent, H_1 and H_2 depend upon the concentrations of chlorine dioxide, malonic acid and iodine. The concentrations of these feed reagents, of course, vary through the gel. We approximate this spatial dependence by assuming that each concentration varies linearly from its reservoir value when it enters the gel to zero at the opposite end of the gel. The spatial dependence of these concentrations and of the functions K', H_1 and H_2 is shown in Fig. 5. The shaded region, in which both inequalities are satisfied and hence Turing structures can arise, is seen to occupy only a small fraction of the length of the gel. In Fig. 6, we compare the predictions of this model with experiments in which, by varying the focal point

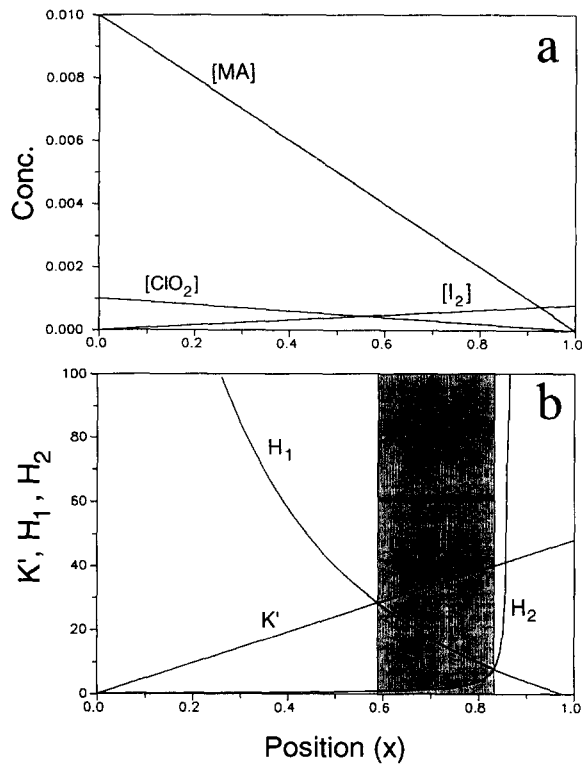

Fig. 5. Concentration gradients imposed by the boundary conditions (a) and position-dependent functions that determine the range of Turing instability in the presence of a gradient (b).

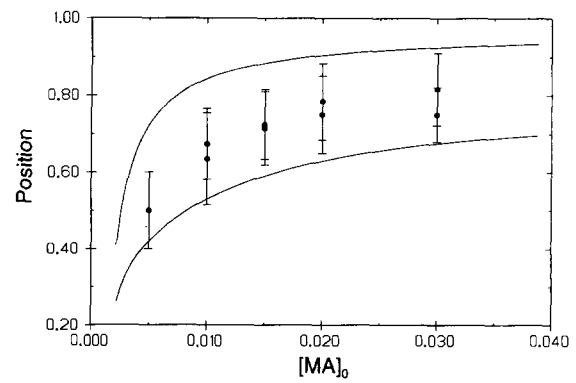

Fig. 6. Dependence of the position of the Turing layer on the concentration of MA. $[ClO_2]_0 = 1 \times 10^{-3}$ M, $[I_2]_0 = 8 \times 10^{-4}$ M, [S] = 3% w/v. Thickness of the gel is 2 mm, normalized from 0 to 1 in the figure. Circles experimental; lines calculated from inequality (8).

of our optical system, we measured the position of the Turing structures in the gel at several different input malonic acid concentrations [22]. The agreement is seen to be excellent.

5. Turing structures in a closed system

Turing's theoretical discussion [16] of reaction–diffusion systems envisioned pattern formation in an initially homogeneous, far-from-equilibrium system in which all parameters were independent of their spatial positions. Experimental necessity caused the first successful Turing experiments [1] to be carried out in a configuration in which important experimental parameters varied over large ranges from one end of the reactor to the other in order that input flows could maintain the system far from equilibrium. Our analysis of the effects of these flows [22], summarized in the previous section, suggests an approach [23] both to generating Turing patterns in a system closer to that described by Turing and to obtaining these structures, albeit transiently, in a closed system convenient for demonstration purposes.

Our model calculations yield values for the input reactant concentrations, $[ClO_2]$, $[I_2]$ and [MA], in the region of the gel where the conditions for Turing structures are satisfied. If we run the reaction in a closed system, e.g., in a petri dish, with initial concentrations chosen to be in this range, it is possible that Turing structures will develop and persist while the concentrations remain within the "Turing range". In Fig. 7, we show a simulation, in a one-dimensional geometry, of batch Turing experiments in the CDIMA system. In an intermediate range of malonic acid concentrations, stationary spatial patterns emerge after an induction period and persist before giving way to bulk oscillation, waves and ultimately to the uniform equilibrium state.

The results of our actual two-dimensional batch experiments are shown in Fig. 8. After an induction period of about 10 min, patterns form and are stationary for up to 30 min. The reactor was two glass plates separated by an 0.5 mm plexiglass spacer. Gel was not used in these experiments. Unfortunately, the structures are visible only at reduced temperatures; 4–5°C is ideal. Thus, we have not quite reached our goal of having a convenient demonstration that can be used at all times of year and in all parts of the world.

6. Future directions

The study of Turing structures has moved rapidly in the four years since their existence was first demonstrated experimentally. At this time, one can point toward several directions in which the field is likely to expand.

We certainly expect that new chemical systems will be found that display Turing patterns. We have suggested a route toward designing such systems in a gel reactor. The likelihood of finding additional catalytic systems is also quite high, since it seems unlikely that the Turing structures observed in the catalytic oxidation of carbon monoxide on platinum [5] depend on any special features of the chemistry in that system. Experiments using other media such as membranes or sol–gel glasses [4] may provide other routes to new systems that give Turing structures.

We have pointed out that experiments thus far have been performed in a geometry that results in quasi-two-dimensional structures, though theory demonstrates that it should be possible to generate three-dimensional structures and that these structures should exhibit a number of interesting features [24,25]. The obstacles to obtaining three-dimensional Turing patterns are primarily technical. Thick layers of gel are difficult to manipulate. Optical methods do not easily lend themselves to observations of three-dimensional structures. The detection problem is likely to be solved by adapting methods from

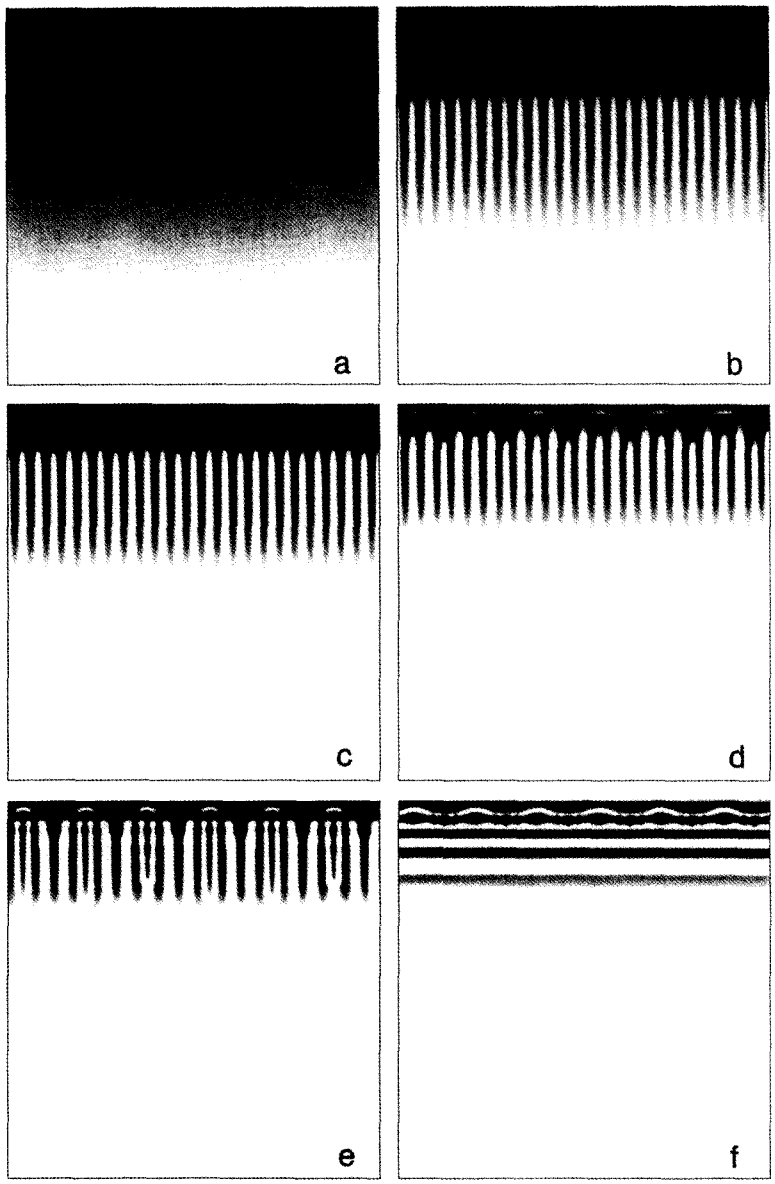

Fig. 7. Model calculations of the time development of transient Turing patterns in a batch reactor using the six-variable model of reactions (1) and (7). $[MA]_0 = 0.0025$ (a), 0.0030 (b), 0.004 (c), 0.005 (d), 0.006 (e), 0.007 (f), $[I_2]_0 = 8.2 \times 10^{-4}$ M, $[ClO_2]_0 = 1 \times 10^{-3}$ M, $[S]_0 = 0.1$ M. Length is 5 mm shown horizontally. Total time is 30 minutes shown vertically. Number of gridpoints is 400. Rate and diffusion constants at 4°C were used. $k_{1a} = 6.2 \times 10^{-4}\,M^{-1}s^{-1}$ and $k_{1b} = 5 \times 10^{-5}$ M at pH = 2, $k_2 = 9.0 \times 10^2\,M^{-1}s^{-1}$, $k_{3a} = 100\,M^{-2}\,s^{-1}$, $k_{3b} = 9.2 \times 10^{-5}\,s^{-1}$, $u = 10^{-14}\,M^2$, $k_7 = 6 \times 10^5\,M^{-2}s^{-1}$, $k_{-7} = 1.0\,s^{-1}$, $D_{ClO_2^-} = D_{ClO_2} = 7.5 \times 10^{-6}$, $D_{I^-} = D_{I_2} = 7.0 \times 10^{-6}$, $D_{MA} = 4.0 \times 10^{-6}$, and $D_{starch} = D_{SI_3^-} = 0\,cm^2\,s^{-1}$. The concentration of starch-triiodide complex was rescaled from 0 to 255 gray levels. Darker means higher concentration of the complex.

other fields. Confocal microscopy and nuclear magnetic resonance imaging are two techniques that suggest themselves for this task.

A great deal is known about the bifurcations of homogeneous dynamical systems, which can be described by sets of ordinary differential equations, particularly for systems that can be modeled with only two or three dependent

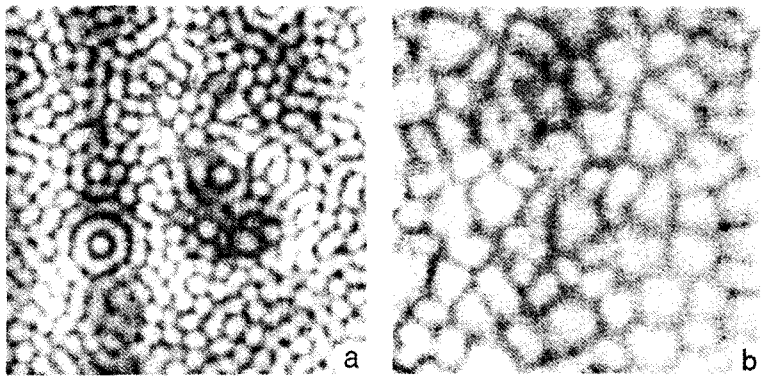

Fig. 8. Mixed spots and stripes (a) and network-like (b) structures in a batch reactor. The wavelength is 0.25 (a) and 0.3 (b) mm. $[ClO_2]_0 = 5 \times 10^{-4}$ M, $[I_2]_0 = 8.0 \times 10^{-4}$ M, $[MA]_0 = 1.0 \times 10^{-3}$ M in (a) and 3.0×10^{-3} M in (b), [Starch] = 1 g/100 ml and [acetic acid] = 10%.

variables [26]. The bifurcation structure of spatiotemporal systems characterized by partial differential equations is far richer and much less well understood. Recent numerical simulations on a simple abstract model [27] show an enormous wealth of spatiotemporal states. Problems that need to be solved include identifying the totality of possible states of a system and the bifurcations between states and developing quantitative measures to characterize a given state. These are not easy tasks, but they are important ones, and we have at our disposal some powerful numerical, analytic and experimental tools with which to tackle them.

Finally, the success of chemists in experimentally characterizing Turing structures is likely to lead not only to advances in the theoretical, mathematical understanding of this phenomenon, but also to experimental progress in other branches of science in which Turing patterns may occur. While the Turing mechanism has been suggested as a route to pattern formation in fields ranging from astrophysics [28] to economics [29], the most fruitful area of investigation is likely to be biology. Increasingly more powerful techniques for obtaining spatially and temporally resolved concentration profiles, for example using calcium-sensitive dyes [30], offer the prospect of identifying the chemical species involved in certain types of biological pattern formation and of evaluating Turing's hypothesis that reaction and diffusion can combine to yield morphogenesis.

7. Conclusions

The similarities between the study of Turing structures today and of oscillating chemical reactions twenty to twenty-five years ago are striking. We summarize some of the parallels in Table 1.

The CIMA reaction has taken on the role of the BZ system – the prototype reaction on which nearly all experimental studies are carried out. Thus far, the CDIMA reaction is the only variant of the CIMA reaction, but just as the BZ system spawned many new chemical oscillators [31,32], we may expect further variants of the CIMA system in the near future. One obvious possibility is to modify the organic reaction kinetics by replacing malonic acid by similar organic species as we have already done in studying the temporal oscillation of the CIMA system [13].

The three-variable Oregonator model [33], which facilitated both numerical and analytical calculations while remaining faithful to the chemistry of the BZ reaction, sparked interest in chemical oscillation. There is some indication that the two-variable model of Eqs. (8) is playing

Table 1
Points of similarity between oscillating reactions and Turing structures

Aspect	Oscillating reactions	Turing structures
prototype system	Belousov–Zhabotinsky (BrO_3^-–metal catalyst–MA)	CIMA (ClO_2^-–I^-–MA)
variations	Uncatalyzed BZ, Briggs–Rauscher	CDIMA
simple, realistic model	Oregonator	Brandeisator
systematic design algorithm	CSTR, cross-shaped phase diagram	CFUR, immobile complex
bifurcation to more complex behavior	Bursting, mixed mode oscillation, chaos	Interaction with Hopf or saddle node bifurcations, spatial turbulence
lecture demonstration	BZ, Briggs–Rauscher	??

a similar though less dramatic role in the study of Turing structures, where several other simple, though less chemically relevant models were already available.

One of the major breakthroughs in the study of chemical oscillators was the introduction of the continuous flow stirred tank reactor [34] as a tool for keeping the system far from equilibrium. By combining the CSTR with a systematic design approach [35] based on a simple, generic, mathematical model [36], it became possible in the 1980s to design literally dozens of new chemical oscillators. As we have seen, the experimental study of Turing structures began with the introduction of continuous unstirred flow reactors. The approach of introducing an immobile complexing agent for the activator species offers a promising route to designing new Turing systems. There may well be other routes.

The temporal oscillations that were studied initially consisted of relatively simple periodic, or nearly periodic behavior with a single peak in each cycle. It soon became apparent, however, that these systems can display far more complex temporal patterns, including multiple peaks in each cycle (mixed-mode oscillation), alternation of active and quiescent periods (bursting), dual-frequency oscillation (quasiperiodicity) and aperiodic oscillations (chaos). The variety of possible spatio-temporal behavior is even vaster and is only beginning to be explored [20,27].

Finally, the striking and easily mounted lecture demonstrations based on the Belousov-Zhabotinsky and Briggs–Rauscher reactions can be given much of the credit for attracting young scientists to the study of nonlinear chemical dynamics. To date there is no such demonstration available to illustrate the Turing phenomenon. In this survey, we have attempted to show how far we have progressed toward the goal of constructing a system that can display Turing patterns under easily accessible conditions, and what still remains to be done.

Acknowledgments

This work was supported by the National Science Foundation (CHE-9023294), the Petroleum Research Fund (25529-AC6) and a U.S.–Hungarian cooperative grant from the NSF (INT-8921816 and INT-9322738) and the Hungarian Academy of Sciences. We thank Sándor Kádár, Kenneth Kustin and Anatol Zhabotinsky for many helpful discussions. We also acknowledge the support of the W.M. Keck Foundation.

References

[1] V. Castets, E. Dulos, J. Boissonade and P. De Kepper, Phys. Rev. Lett. 64 (1990) 2953.
[2] B.Z. Shakhashiri, Chemical Demonstrations, Vol. 2 (The University of Wisconsin Press, 1983).
[3] Q. Ouyang and H.L. Swinney, Nature 352 (1991) 610.
[4] I.R. Epstein, I. Lengyel, S. Kádár, M. Kagan and M. Yokoyama, Physica A 188 (1992) 26.
[5] S. Jakubith, H.H. Rothermund, W. Engel, A. von Oertzen and G. Ertl, Phys. Rev. Lett. 65 (1990) 3013.

[6] P. De Kepper, I.R. Epstein, K. Kustin and M. Orbán, J. Phys. Chem. 86 (1982) 170.
[7] D.M. Kern and C.-H. Kim, J. Am. Chem. Soc. 87 (1965) 5309.
[8] J.D. Meeus and J. Sigalla, J. Chim. Phys. Phys.-Chim. Biol. 63 (1966) 453.
[9] I.R. Epstein and K. Kustin, J. Phys. Chem. 89 (1985) 2275.
[10] O. Citri and I.R. Epstein, J. Phys. Chem. 91 (1987) 6034.
[11] I.R. Epstein and M. Orbán, in: Oscillations and Travelling Waves in Chemical Systems, eds. R.J. Field and M. Burger (Wiley, New York, 1985) p. 257.
[12] G. Rábai and M.T. Beck, Inorg. Chem. 26 (1987) 1195.
[13] I. Lengyel, G. Rábai and I.R. Epstein, J. Am. Chem. Soc. 112 (1990) 9104.
[14] I. Lengyel and I.R. Epstein, Science 251 (1991) 650.
[15] A.A. Andronov, E.A. Vitt and S.E. Khaiken, Nonlinear Oscillations (Pergamon, Oxford, 1966) p. 361.
[16] A.M. Turing, Phil. Trans. Roy. Soc. London B 237 (1952) 37.
[17] J.D. Murray, Mathematical Biology (Springer-Verlag, Berlin, 1989).
[18] I. Lengyel and I.R. Epstein, Proc. Nat. Acad. Sci. USA 89 (1992) 3977.
[19] E.C. Edblom, M. Orbán and I.R. Epstein, J. Am. Chem. Soc. 108 (1986) 2826.
[20] K.J. Lee, W.D. McCormick, Q. Ouyang and H.L. Swinney, Science 261 (1993) 192.
[21] G. Rábai, M. Orbán and I.R. Epstein, Acc. Chem. Res. 23 (1990) 258.
[22] I. Lengyel S. Kádár and I.R. Epstein, Phys. Rev. Lett. 69 (1992) 2729.
[23] I. Lengyel, S. Kádár and I.R. Epstein, Science 259 (1993) 493.
[24] D. Walgraef, G. Dewel and P. Borckmans, J. Chem. Phys. 78 (1983) 3043.
[25] A. De Wit, G. Dewel, P. Borckmans and D. Walgraef, Physica D 61 (1992) 289.
[26] J. Guckenheimer and P. Holmes, Nonlinear Oscillations, Dynamical Systems, and Bifurcations of Vector Fields, Applied Mathematical Sciences, Vol. 42 (Springer, Berlin, 1983).
[27] J.E. Pearson, Science 261 (1993) 189.
[28] T. Nozakura and S. Ikeuchi, Astrophys. J. 279 (1984) 40.
[29] M. Maruyama, Amer. Sci. 51 (1963) 164.
[30] J. Lechleiter, S. Girard, E. Peralta and D. Chapman, Science 252 (1991) 123.
[31] M. Orbán and E. Kőrös, J. Phys. Chem. 82 (1978) 1672.
[32] T.S. Briggs and W.C. Rauscher, J. Chem. Ed. 50 (1973) 496.
[33] R.J. Field and R.M. Noyes, J. Chem. Phys. 60 (1974) 1877.
[34] A. Pacault, P. Hanusse, P. De Kepper, C. Vidal and J. Boissonade, Acc. Chem. Res. 9 (1976) 438.
[35] I.R. Epstein, K. Kustin, P. De Kepper and M. Orbán, Sci. Amer. 248 (1983) 112.
[36] J. Boissonade and P. De Kepper, J. Phys. Chem. 84 (1980) 501.